International Journal of Science and Research (IJSR)
ISSN (Online): 2319-7064
Index Copernicus Value (2013): 6.14 | Impact Factor (2013): 4.438

# Scattering of Gaussian Beam from a Perfect Electromagnetic Conductor (PEMC) Spheroid Coated by Dielectric Material

**Bushra Anam Khalil[1], Muhammad Waqas Munir[2], Syed Ali Shahid[3]**

[1]University of Agriculture Faisalabad, Department of Physics, University Road, Faisalabad 38000, Pakistan

[2]Teesside University, School of Science and Engineering, Middlesbrough, Tees Valley, TS1 3BA, UK

[3]Islam College of Engineering and Management Sciences-UET, Department of Electrical Engineering

**Abstract:** ***This research paper presents an exact analytic solution to the problem of Scattering of Gaussian beam by a Perfect Electromagnetic Conductor (PEMC) spheroid coated by a dielectric material using Mie theory. Perfect Electromagnetic Conductor (PEMC) medium is used as a special type of meta-material which is a generalization of the well-known concepts of Perfect Electric Conductor (PEC) and Perfect Magnetic Conductor (PMC). One of the basic characteristics of PEMC medium is its admittance type parameter M. This parameter acts as a basis in deciding the natures of medium as the PEC or PMC. The analytical expressions were derived in terms of spheroidal vector wave functions, for exploring the incident, scattered and transmitted Gaussian beam fields. Scattering and transmission coefficients were obtained by using boundary conditions at free space-dielectric and dielectric-PEMC interfaces. However, these coefficients were used to calculate the radar cross section (Backscattering cross section) and Bi-static cross section of Perfect Electromagnetic Conductor (PEMC). Backscattering cross section and Bi-static cross section were also discussed by effect of parameter M. The result obtained in this investigation were compared with the unveil data to verify the validity of the analytical expressions.***

**Keywords:** Gaussian beam, Perfect electromagnetic conductor, Dielectric material, Backscattering cross section.

## 1. Introduction

A perfect conductor may be defined as a material or medium in which the charge can flow freely. So it can be said that a perfect conductor has an infinite value of conductivity and a zero resistivity. It is purely an idealization of material used in most theoretical studies. Basically there exist two types of perfect conductors as perfect electric conductor (PEC) and perfect magnetic conductor (PMC).

### 1.1 Perfect Electric Conductor (PEC)

While studying materials or mediums in electrostatics, one of the most important assumptions made is that within a perfect electric conductor (PEC) the charges are in equilibrium and are fixed in space inside the medium. As a result, electric field intensity E becomes zero inside PEC and all the points in it are considered to be at same potential. So a perfect electric conductor (PEC) is said to be an equi-potential. In the absence of an external electric field, the charges inside PEC are arranged so as to vanish the internal electrostatic field intensity. When this conductor is placed in an external electric field, a temporary flow of charges occurs. By the end of this flow, charges make their arrangement in such a way so that an internal field is established inside the PEC in order to add up with the external field and produces a resultant zero field. It can be said that the external field is distorted by the charges present inside PEC [3].

**E = 0** inside the perfect electric conductor (PEC), so by Faraday's law **B = 0**. These results can be interpreted for a perfect electric conductor (PEC) as under:

$$\mathbf{E} = \frac{1}{\epsilon}\mathbf{D} \quad \& \; \mathbf{B} = \mu\mathbf{H} \tag{1.1}$$

Putting values of **E** and **B** in above equation set gives:

$$\epsilon = \infty \;\; \& \; \mu = 0 \tag{1.2}$$

Perfect electric conductor (PEC) has its own characteristic boundary conditions, which can be mathematically stated as under:

$$\mathbf{n} \times \mathbf{E} = 0 \quad , \quad \mathbf{n}.\mathbf{B} = 0 \tag{1.3}$$

Where **n** is the unit normal vector.

### 1.2 Perfect Magnetic Conductor (PMC)

The idealization of perfect magnetic conductor (PMC) is analogous to perfect electric conductor (PEC) in electromagnetic. The difference between both is that in PEC electric field intensity is zero while in PMC magnetic field intensity is zero. This happens by the arrangement of magnetic dipoles inside the conductor so as to vanish the internal magnetic field. All the basic conditions for the material to be a perfect conductor, as discussed previously, are also satisfied for perfect magnetic conductor (PMC) [5]

**H = 0** inside the perfect magnetic conductor (PMC), so by Maxwell's equations **D = 0**. These results can be interpreted for a perfect magnetic conductor (PMC) as under:

$$\mathbf{E} = \frac{1}{\epsilon}\mathbf{D} \quad \& \; \mathbf{B} = \mu\mathbf{H} \tag{1.4}$$

Putting values of **H** and **D** in above equation set gives;

$$\epsilon = 0 \;\; \& \; \mu = \infty \tag{1.5}$$

Perfect magnetic conductor (PMC) is also specified by its boundary conditions as below:

$$\mathbf{n} \times \mathbf{H} = 0 \quad , \ \mathbf{n}.\mathbf{D} = 0 \qquad (1.6)$$

### 1.3 Perfect Electromagnetic Conductor (PEMC)

Perfect electromagnetic conductors (PEMC) are meta-materials having properties which are not commonly observed in naturally existing materials. For perfect magnetic conductor (PMC) and perfect electric conductor (PEC) cross-polarized component of scattered field vanishes, however for perfect electromagnetic conductor (PEMC) both co-polarized and cross-polarized components of the reflected wave or field exist. As it is discussed in previous sections that in perfect electric conductor (PEC) electric field E vanishes and in perfect magnetic conductor (PMC) magnetic field H vanishes. Perfect electromagnetic conductors (PEMC) also possess boundary conditions, which can be mathematically stated as under [7] [2].

$$\mathbf{n} \times (\mathbf{H} + M\mathbf{E}) = 0 \ , \ \ \mathbf{n}.(\mathbf{D} - M\mathbf{B}) = 0 \qquad (1.7)$$

Where **M** denotes the admittance of the PEMC boundary and is independent of spatial coordinates. From these boundary conditions it is can easily be understood that PEMC matches the PMC when **M = 0**, while it becomes the PEC for $M \to \pm\infty$. Perfect electromagnetic conductor (PEMC) is a medium where the linear combination of E and H vanishes. These boundary conditions can be used to find out the required solutions of the electromagnetic field interacting with the PEMC material in any geometry. In order to fulfill the boundary conditions, co-polarized as well as cross-polarized field components are required to represent the field. This fact provides the base for the assumption in case of PEMC that it possesses a non-reciprocal feature.

When PEMC material is represented in differential form, it is found as the simplest probable medium [2]. It has been verified theoretically that a PEMC material acts as a perfect reflector of electromagnetic waves [4]. The difference between PEMC and PMC or PEC is that the reflected wave has a cross-polarized component. These incident and scattered field can be expressed in terms of appropriate products of Bessel/Hankel functions and Legendre polynomials.

## 2. Scattering theory for coated PEMC spheroid

Consider the geometry of a prolate PEMC spheroid with prolate spheroidal coordinates $(\zeta, \eta, \phi)$ which is coated by a spheroidal shell, so that the external coordinates are $(\zeta_1, \eta, \phi)$ and is centered at the origin O. The permittivity of the shell material is $\varepsilon_1 = \varepsilon_r \varepsilon_0$ and its permeability is $\mu_1 = \mu_r \mu_0$, where $\varepsilon_0$ and $\mu_0$ are the free space permittivity and permeability, respectively. Incident Gaussian beam makes an angle $\theta$ with y-axis and angle $\varphi$ with the xz plane. Similarly Scattered Gaussian beam makes an angle (scattering angle) with y-axis and an angle $\varphi$ with the scattering plane zx.

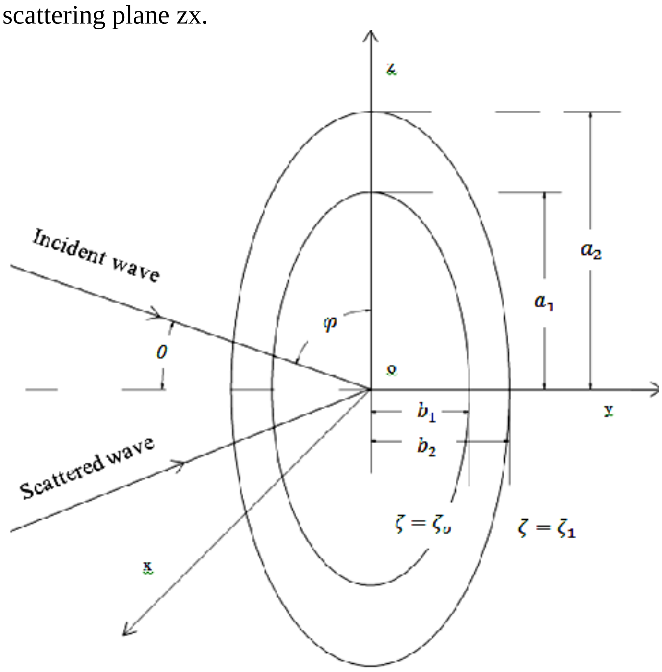


**Figure 1:** Coated perfect electromagnetic conductor (PEMC) spheroid illuminated by Gaussian Beam.

### 2.1 Speroidal vector wave functions

The Gaussian beam field will be expanded in terms of the spheroidal vector wave functions:

Values of $\eta$ and $\phi$ component of M:

$$M^{r(i)}_{\substack{e\\o}mn\eta}(c;\eta,\zeta,\phi) = \frac{m\zeta}{(\zeta^2 \pm \eta^2)^{\frac{1}{2}}(1-\eta^2)^{\frac{1}{2}}} S_{mn} R^{(i)}_{mn} \, {}_{(-\cos)}^{\sin}(m\phi) \quad (2.1)$$

$$M^{r(i)}_{\substack{e\\o}mn\phi}(c;\eta,\zeta,\phi) = \frac{(\zeta^2 \pm 1)^{\frac{1}{2}}(1-\eta^2)^{\frac{1}{2}}}{\zeta^2 \pm \eta^2} \left[\zeta \frac{dS_{mn}}{d\eta} R^{(i)}_{mn} \pm \eta S_{mn} \frac{dR^{(i)}_{mn}}{d\zeta}\right] {}_{\sin}^{\cos}(m\phi) \qquad (2.2)$$

Values of $\eta$ and $\phi$ component of N:

$$N^{r(i)}_{\substack{e\\o}mn\eta}(c;\eta,\zeta,\phi) = \frac{2(1-\eta^2)^{\frac{1}{2}}}{kd(\zeta^2 \pm \eta^2)^{\frac{1}{2}}} \left[\frac{dS_{mn}}{d\eta}\frac{\partial}{\partial\xi}\left(\frac{\zeta(\zeta^2 \pm 1)}{\zeta^2 \pm \eta^2} R^{(i)}_{mn}\right) \pm \eta S_{mn} \frac{\partial}{\partial\zeta}\left(\frac{\zeta(\zeta^2 \pm 1)}{\zeta^2 \pm \eta^2}\frac{dR^{(i)}_{mn}}{d\zeta}\right) \mp \frac{\eta}{(1-\eta^2)(\zeta^2 \pm 1)} S_{mn} R^{(i)}_{mn}\right] {}_{\sin}^{\cos}(m\phi) \qquad (2.3)$$

$$N^{r(i)}_{\substack{e\\o}mn\phi}(c;\eta,\zeta,\phi) = \frac{2(1-\eta^2)^{\frac{1}{2}}(\zeta^2 \pm 1)^{\frac{1}{2}}}{kd(\zeta^2 \pm \eta^2)} \left[\frac{\pm 1}{\zeta^2 \pm 1}\frac{d}{d\eta}(\eta S_{mn}) R^{(i)}_{mn} - \frac{1}{1-\eta^2} S_{mn} \frac{d}{d\zeta}\left(\zeta R^{(i)}_{mn}\right) {}_{(-\cos)}^{\sin}(m\phi)\right] \qquad (2.4)$$

Here spherical coordinates$(\zeta, \eta, \phi)$ are used, and the subscript *e* stands for even and *o* for odd, according to whether $\cos(m\phi)$ or $\sin(m\phi)$ is used when multiplying by Radial function $R_{mn}$ and angular function $S_{mn}$. The wave number *k* is given by $k_1 = \omega\sqrt{\epsilon_1 \mu_1}$ inside the coating, and by $k_o = \omega\sqrt{\epsilon_o \mu_o}$ outside it. The superscript $i$ specifies the


www.ijsr.net

Paper ID: SUB151814

choice of the radial function $z_n(kr)$. For $i = 1$ this is a spherical Bessel function $j_n(kr)$, for $i = 2$ a spherical Neumann function $n_n(kr)$, and for $i = 3$ a spherical Hankel function $h_n(kr)$. A Gaussian beam of frequency $\omega$, propagating in the $z$ direction, with the electric field polarized in the $x$ direction, is incident on the spheroid.

### 2.2 Incident Field

The expansion of the incident field is given by [6].

$$E^{\iota} = E_o \sum_{n=1}^{\infty} \iota^n \frac{2n+1}{n(n+1)} \left[G_{nTE}\, M_{o1n}^{(1)} - \iota G_{nTM} N_{e1n}^{(1)}\right] \qquad (2.5)$$

$$H^{\iota} = -\left(\frac{E_o}{\eta_o}\right) \sum_{n=1}^{\infty} \iota^n \frac{2n+1}{n(n+1)} \left[G_{nTM}\, M_{e1n}^{(1)} + \iota G_{nTE} N_{o1n}^{(1)}\right] \qquad (2.6)$$

Where

$$\eta_o = \sqrt{\mu_o/\varepsilon_o}$$

### 2.3 Scattered field

The scattered field in the region $\zeta > \zeta_1$ is expanded in the form

$$E^s = E_o \sum_{n=1}^{\infty} \iota^n \frac{2n+1}{n(n+1)} \left[a_n^s\, M_{o1n}^{(3)} + c_n^s M_{e1n}^{(3)} - \iota b_n^s N_{e1n}^{(3)} - \iota d_n^s N_{o1n}^{(3)}\right] \qquad (2.7)$$

$$H^s = -\left(\frac{E_o}{\eta_o}\right) \sum_{n=1}^{\infty} \iota^n \frac{2n+1}{n(n+1)} \left[b_n^s\, M_{e1n}^{(3)} + d_n^s M_{o1n}^{(3)} + \iota a_n^s N_{o1n}^{(3)} + \iota c_n^s N_{e1n}^{(3)}\right] \qquad (2.8)$$

In the standard Mie type scattering theory only the coefficients $a_n^s$ and $b_n^s$ are needed in the scattered field expansion. Since in the PEMC boundary conditions (1) and (2) mixing of **E** and **H** occurs; the coefficients $c_n^s$ and $d_n^s$ have to be added. These represent the cross polarized components of the scattered field.

### 2.4 Transmitted Field

The fields inside the coating are expanded in the form

$$E^t = E_o \sum_{n=1}^{\infty} \iota^n \frac{2n+1}{n(n+1)} \left[a_n^{t1}\, M_{o1n}^{(1)} + a_n^{t2}\, M_{o1n}^{(2)} + c_n^{t1} M_{e1n}^{(1)} + c_n^{t2} M_{e1n}^{(2)} - \iota b_n^{t1} N_{e1n}^{(1)} - \iota b_n^{t2} N_{e1n}^{(2)} - \iota d_n^{t1} N_{o1n}^{(1)} - \iota d_n^{t2} N_{o1n}^{(2)}\right] \qquad (2.9)$$

$$H^t = -\left(\frac{E_o}{\eta_1^*}\right) \sum_{n=1}^{\infty} \iota^n \frac{2n+1}{n(n+1)} \left[b_n^{t1}\, M_{e1n}^{(1)} + b_n^{t2}\, M_{e1n}^{(2)} + d_n^{t1} M_{o1n}^{(1)} + d_n^{t2} M_{o1n}^{(2)} + \iota a_n^{t1} N_{o1n}^{(1)} + \iota a_n^{t2} N_{o1n}^{(2)} + \iota c_n^{t1} N_{e1n}^{(1)} + \iota c_n^{t2} N_{e1n}^{(2)}\right] \qquad (2.10)$$

Where

$$\eta_1^* = \sqrt{\mu_1/\varepsilon_1}$$

## 3. Boundary conditions

We know apply the boundary conditions at the interface (dielectric-PEMC). At $\zeta = \zeta_o$ the tangential components have to satisfy the boundary conditions

$$H_\eta^t + ME_\eta^t = 0 \quad , \quad H_\phi^t + ME_\phi^t = 0 \qquad (3.1)$$

Similarly by using other boundary conditions at free space-dielectric interface at $\zeta = \zeta_1$

$$H_\phi^i + H_\phi^s = H_\phi^t \quad , \quad H_\eta^i + H_\eta^s = H_\eta^t \qquad (3.2)$$

$$E_\phi^i + E_\phi^s = E_\phi^t \quad , \quad E_\eta^i + E_\eta^s = E_\eta^t \qquad (3.3)$$

### 3.1 Boundary conditions implementations

Applying the boundary conditions (3.1) – (3.3) and using the orthogonality properties of the angular functions we obtain the system of six linear equations.

$$b_n^{t1} R_{1m}^1 + b_n^{t2} R_{1m}^2 - \eta_1^* M c_n^{t1} R_{1m}^1 - \eta_1^* M c_n^{t2} R_{1m}^2 = 0 \qquad (3.4)$$

$$c_n^{t1}\left[\frac{dS_{1n}}{d\eta}\frac{\partial}{\partial\zeta}\left(\frac{\zeta(\zeta^2+1)}{\zeta^2+\eta^2}R_{1n}^{(1)}\right) + \eta S_{1n}\frac{\partial}{\partial\xi}\left(\frac{\zeta(\zeta^2+1)}{\zeta^2+\eta^2}\frac{dR_{1n}^{(1)}}{d\zeta}\right) - \frac{\eta}{(1-\eta^2)(\zeta^2+1)}S_{1n}R_{1n}^{(1)}\right] + c_n^{t1}\left[\frac{dS_{1n}}{d\eta}\frac{\partial}{\partial\zeta}\left(\frac{\zeta(\zeta^2+1)}{\zeta^2+\eta^2}R_{1n}^{(1)}\right) + \eta S_{1n}\frac{\partial}{\partial\zeta}\left(\frac{\zeta(\zeta^2+1)}{\zeta^2+\eta^2}\frac{dR_{1n}^{(1)}}{d\zeta}\right) - \frac{\eta}{(1-\eta^2)(\zeta^2+1)}S_{1n}R_{1n}^{(1)}\right]$$

$$+M\eta_1^*\left\{b_n^{t1}\left[\frac{dS_{1n}}{d\eta}\frac{\partial}{\partial\zeta}\left(\frac{\zeta(\zeta^2+1)}{\zeta^2+\eta^2}R_{1n}^{(1)}\right) + \eta S_{1n}\frac{\partial}{\partial\xi}\left(\frac{\zeta(\zeta^2+1)}{\zeta^2+\eta^2}\frac{dR_{1n}^{(1)}}{d\zeta}\right) - \frac{\eta}{(1-\eta^2)(\zeta^2+1)}S_{1n}R_{1n}^{(1)}\right] + b_n^{t2}\left[\frac{dS_{1n}}{d\eta}\frac{\partial}{\partial\zeta}\left(\frac{\zeta(\zeta^2+1)}{\zeta^2+\eta^2}R_{1n}^{(2)}\right) + \eta S_{1n}\frac{\partial}{\partial\zeta}\left(\frac{\zeta(\zeta^2+1)}{\zeta^2+\eta^2}\frac{dR_{1n}^{(2)}}{d\zeta}\right) - \frac{\eta}{(1-\eta^2)(\zeta^2+1)}S_{1n}R_{1n}^{(2)}\right]\right\} = 0 \qquad (3.5)$$

$$\eta_o b_n^{t1} R_{1n}^{(1)} + \eta_o b_n^{t2} R_{1n}^{(2)} - \eta_1^* b_n^s R_{1n}^{(3)} = \eta_1^* G_{nTM} S_{1n} R_{1n}^1 \qquad (3.6)$$

$$\eta_o c_n^{t1}\left[\frac{dS_{mn}}{d\eta}\frac{\partial}{\partial\zeta}\left(\frac{\zeta(\zeta^2+1)}{\zeta^2+\eta^2}R_{mn}^{(1)}\right) + \eta S_{mn}\frac{\partial}{\partial\xi}\left(\frac{\zeta(\zeta^2+1)}{\zeta^2+\eta^2}\frac{dR_{mn}^{(1)}}{d\zeta}\right) - \frac{\eta}{(1-\eta^2)(\zeta^2+1)}S_{mn}R_{mn}^{(1)}\right] + \eta_o c_n^{t2}\left[\frac{dS_{mn}}{d\eta}\frac{\partial}{\partial\zeta}\left(\frac{\zeta(\zeta^2+1)}{\zeta+\eta^2}R_{mn}^{(2)}\right) + \eta S_{mn}\frac{\partial}{\partial\zeta}\left(\frac{\zeta(\zeta+1)}{\zeta^2+\eta^2}\frac{dR_{mn}^{(2)}}{d\zeta}\right) - \frac{\eta}{(1-\eta^2)(\zeta^2+1)}S_{mn}R_{mn}^{(2)}\right] = \eta_1^* c_n^s\left[\frac{dS_{mn}}{d\eta}\frac{\partial}{\partial\zeta}\left(\frac{\zeta(\zeta^2+1)}{\zeta^2+\eta^2}R_{mn}^{(3)}\right) + \eta S_{mn}\frac{\partial}{\partial\xi}\left(\frac{\zeta(\zeta^2+1)}{\zeta^2+\eta^2}\frac{dR_{mn}^{(3)}}{d\zeta}\right) - \frac{\eta}{(1-\eta^2)(\zeta^2+1)}S_{mn}R_{mn}^{(3)}\right] \qquad (3.7)$$

$$c_n^{t1} R_{1n}^{(1)} + c_n^{t2} R_{1n}^{(2)} - c_n^s R_{1n}^{(3)} = 0 \qquad (3.8)$$

$$\frac{G_{nTM}}{k_o}\left[\frac{dS_{1n}}{d\eta}\frac{\partial}{\partial\zeta}\left(\frac{\zeta(\zeta^2+1)}{\zeta^2+\eta^2}R_{1n}^{(1)}\right) + \eta S_{1n}\frac{\partial}{\partial\zeta}\left(\frac{\zeta(\zeta^2+1)}{\zeta^2+\eta^2}\frac{dR_{1n}^{(1)}}{d\zeta}\right) - \frac{\eta}{(1-\eta^2)(\zeta^2+1)}S_{1n}R_{1n}^{(1)}\right] + \frac{b_n^s}{k_o}\left[\frac{dS_{1n}}{d\eta}\frac{\partial}{\partial\zeta}\left(\frac{\zeta(\zeta^2+1)}{\zeta^2+\eta^2}R_{1n}^{(3)}\right) + \eta S_{1n}\frac{\partial}{\partial\zeta}\left(\frac{\zeta(\zeta^2+1)}{\zeta^2+\eta^2}\frac{dR_{1n}^{(3)}}{d\zeta}\right) - \frac{\eta}{(1-\eta^2)(\zeta^2+1)}S_{1n}R_{1n}^{(3)}\right] =$$

$$\frac{b_n^{t1}}{k_1}\left[\frac{dS_{1n}}{d\eta}\frac{\partial}{\partial\zeta}\left(\frac{\zeta(\zeta^2+1)}{\zeta^2+\eta^2}R_{1n}^{(1)}\right)+\eta S_{1n}\frac{\partial}{\partial\zeta}\left(\frac{\zeta(\zeta^2+1)}{\zeta^2+\eta^2}\frac{dR_{1n}^{(1)}}{d\zeta}\right)-\frac{\eta}{(1-\eta^2)(\zeta^2+1)}S_{1n}R_{1n}^{(1)}\right]+\frac{b_n^{t2}}{k_1}\left[\frac{dS_{1n}}{d\eta}\frac{\partial}{\partial\zeta}\left(\frac{\zeta(\zeta^2+1)}{\zeta^2+\eta^2}R_{1n}^{(2)}\right)+\eta S_{1n}\frac{\partial}{\partial\zeta}\left(\frac{\zeta(\zeta^2+1)}{\zeta^2+\eta^2}\frac{dR_{1n}^{(2)}}{d\zeta}\right)-\frac{\eta}{(1-\eta^2)(\zeta^2+1)}S_{1n}R_{1n}^{(2)}\right] \tag{3.9}$$

For the six coefficients $b_n^s, b_n^{t1}, b_n^{t2}, c_n^s, c_n^{t1}, c_n^{t2}$. Furthermore, the system of six linear equations

$$\frac{d_n^{t1}}{k_1}\left[\frac{dS_{1n}}{d\eta}\frac{\partial}{\partial\zeta}\left(\frac{\zeta(\zeta^2-1)}{\zeta^2-\eta^2}R_{1n}^{(1)}\right)-\eta S_{1n}\frac{\partial}{\partial\zeta}\left(\frac{\zeta(\zeta^2-1)}{\zeta^2-\eta^2}\frac{dR_{1n}^{(1)}}{d\xi}\right)+\frac{\eta}{(1-\eta^2)(\zeta^2-1)}S_{1n}R_{1n}^{(1)}\right]+\frac{d_n^{t2}}{k_1}\left[\frac{dS_{1n}}{d\eta}\frac{\partial}{\partial\zeta}\left(\frac{\zeta(\zeta^2-1)}{\zeta^2-\eta^2}R_{1n}^{(2)}\right)-\eta S_{1n}\frac{\partial}{\partial\xi}\left(\frac{\zeta(\zeta^2-1)}{\zeta^2-\eta^2}\frac{dR_{1n}^{(2)}}{d\xi}\right)+\frac{\eta}{(1-\eta^2)(\zeta^2-1)}S_{1n}R_{1n}^{(2)}\right]-\frac{d_n^s}{k_o}\left[\frac{dS_{1n}}{d\eta}\frac{\partial}{\partial\zeta}\left(\frac{\zeta(\zeta^2-1)}{\zeta^2-\eta^2}R_{1n}^{(3)}\right)-\eta S_{1n}\frac{\partial}{\partial\zeta}\left(\frac{\zeta(\zeta^2-1)}{\zeta^2-\eta^2}\frac{dR_{1n}^{(3)}}{d\zeta}\right)+\frac{\eta}{(1-\eta^2)(\zeta^2-1)}S_{1n}R_{1n}^{(3)}\right]=0 \tag{3.10}$$

$$a_n^{t1}R_{1n}^{(1)}+a_n^{t2}R_{1n}^{(2)}-a_n^sR_{1n}^{(3)}=G_{nTE}R_{1n}^{(1)} \tag{3.11}$$

$$d_n^{t1}R_{1m}^1+d_n^{t2}R_{1m}^2-M\eta_1^*a_n^{t1}R_{1m}^1-M\eta_1^*a_n^{t2}R_{1m}^2=0 \tag{3.12}$$

$$a_n^{t1}\left[\frac{dS_{1n}}{d\eta}\frac{\partial}{\partial\zeta}\left(\frac{\zeta(\zeta^2-1)}{\zeta^2-\eta^2}R_{1n}^{(1)}\right)-\eta S_{1n}\frac{\partial}{\partial\zeta}\left(\frac{\zeta(\zeta^2-1)}{\zeta^2-\eta^2}\frac{dR_{1n}^{(1)}}{d\zeta}\right)+\frac{\eta}{(1-\eta^2)(\zeta^2-1)}S_{1n}R_{1n}^{(1)}\right]+a_n^{t2}\left(\left[\frac{dS_{1n}}{d\eta}\frac{\partial}{\partial\zeta}\left(\frac{\zeta(\zeta^2-1)}{\zeta^2-\eta^2}R_{1n}^{(2)}\right)-\eta S_{1n}\frac{\partial}{\partial\zeta}\left(\frac{\zeta(\zeta^2-1)}{\zeta^2-\eta^2}\frac{dR_{mn}^{(2)}}{d\zeta}\right)+\frac{\eta}{(1-\eta^2)(\zeta^2-1)}S_{1n}R_{1n}^{(2)}\right]\right)$$

$$+M\eta_1^*\left\{d_n^{t1}\left[\frac{dS_{1n}}{d\eta}\frac{\partial}{\partial\zeta}\left(\frac{\zeta(\zeta^2-1)}{\zeta^2-\eta^2}R_{1n}^{(1)}\right)-\eta S_{1n}\frac{\partial}{\partial\xi}\left(\frac{\zeta(\zeta^2-1)}{\zeta^2-\eta^2}\frac{dR_{1n}^{(1)}}{d\xi}\right)+\frac{\eta}{(1-\eta^2)(\zeta^2-1)}S_{1n}R_{1n}^{(1)}\right]+d_n^{t1}\left[\frac{dS_{1n}}{d\eta}\frac{\partial}{\partial\zeta}\left(\frac{\zeta(\zeta^2-1)}{\zeta^2-\eta^2}R_{1n}^{(1)}\right)-\eta S_{1n}\frac{\partial}{\partial\xi}\left(\frac{\zeta(\zeta^2-1)}{\zeta^2-\eta^2}\frac{dR_{1n}^{(1)}}{d\zeta}\right)+\frac{\eta}{(1-\eta^2)(\zeta^2-1)}S_{1n}R_{1n}^{(1)}\right]\right\} \tag{3.13}$$

$$\eta_1^*G_{nTE}\left[\frac{dS_{1n}}{d\eta}\frac{\partial}{\partial\zeta}\left(\frac{\zeta(\zeta^2-1)}{\zeta^2-\eta^2}R_{1n}^{(1)}\right)-\eta S_{mn}\frac{\partial}{\partial\zeta}\left(\frac{\zeta(\zeta^2-1)}{\zeta^2-\eta^2}\frac{dR_{1n}^{(1)}}{d\zeta}\right)+\frac{\eta}{(1-\eta^2)(\xi^2-1)}S_{1n}R_{1n}^{(1)}\right]+\eta_1^*a_n^s\left[\frac{dS_{1n}}{d\eta}\frac{\partial}{\partial\zeta}\left(\frac{\zeta(\zeta^2-1)}{\zeta^2-\eta^2}R_{1n}^{(3)}\right)-\eta S_{mn}\frac{\partial}{\partial\zeta}\left(\frac{\zeta(\zeta^2-1)}{\zeta^2-\eta^2}\frac{dR_{1n}^{(3)}}{d\zeta}\right)+\frac{\eta}{(1-\eta^2)(\zeta^2-1)}S_{1n}R_{1n}^{(3)}\right]$$

$$=\eta_o a_n^{t1}\left[\frac{dS_{1n}}{d\eta}\frac{\partial}{\partial\zeta}\left(\frac{\zeta(\zeta^2-1)}{\zeta^2-\eta^2}R_{1n}^{(1)}\right)-\eta S_{mn}\frac{\partial}{\partial\zeta}\left(\frac{\zeta(\zeta^2-1)}{\zeta^2-\eta^2}\frac{dR_{1n}^{(1)}}{d\xi}\right)+\frac{\eta}{(1-\eta^2)(\zeta^2-1)}S_{1n}R_{1n}^{(1)}\right]+\eta_o a_n^{t2}\left[\frac{dS_{1n}}{d\eta}\frac{\partial}{\partial\xi}\left(\frac{\xi(\xi^2-1)}{\xi^2-\eta^2}R_{1n}^{(2)}\right)-\eta S_{mn}\frac{\partial}{\partial\zeta}\left(\frac{\zeta(\zeta^2-1)}{\zeta^2-\eta^2}\frac{dR_{1n}^{(2)}}{d\xi}\right)+\frac{\eta}{(1-\eta^2)(\zeta^2-1)}S_{1n}R_{1n}^{(2)}\right] \tag{3.14}$$

$$\eta_1^*d_n^sR_{1n}^{(3)}-\eta_o d_n^{t1}R_{1n}^{(1)}-\eta_o d_n^{t2}R_{1n}^{(2)}=0 \tag{3.15}$$

Two systems of six linear equations will be used to obtain two sets of coefficients $a_n^s, a_n^{t1}, a_n^{t2}, d_n^s, d_n^{t1}, d_n^{t2}$ and $b_n^s, b_n^{t1}, b_n^{t2}, c_n^s, c_n^{t1}, c_n^{t2}$.

Electromagnetic waves, with any specified polarization, are normally diffracted or scattered in all directions when incident on a target. These scattered waves are broken down into two parts. The first part is made of waves that have the same polarization as the receiving antenna. The other portion of the scattered waves will have a different polarization to which the receiving antenna does not respond. The two polarizations are orthogonal and are referred to as the Principle Polarization (PP) and Orthogonal Polarization (OP), respectively. The intensity of the backscattered energy that has the same polarization as the radar's receiving antenna is used to define the target RCS.

When a target is illuminated by RF energy, it acts like an antenna, and will have near and far fields. Waves reflected and measured in the near field are, in general, spherical. Alternatively, in the far field the wave fronts are decomposed into a linear combination of plane waves.

The RCS defined above is often referred to as either the monostatic RCS, the backscattered RCS, or simply target RCS. The backscattered RCS is measured from all waves scattered in the direction of the radar and has the same polarization as the receiving antenna. It represents a portion of the total scattered target RCS $\sigma_t$, where $\sigma_t > \sigma$. Assuming spherical coordinate system defined by $(\rho, \theta, \varphi)$ then at range $\rho$ the target scattered cross section is a function of $(\theta, \varphi)$. Let the angles $(\theta_i, \varphi_i)$ define the direction of propagation of the incident waves. Also, let the angles $(\theta_s, \varphi_s)$ define the direction of propagation of the scattered waves. The special case, when $\theta_i = \theta_s$ and $\varphi_i = \varphi_s$, defines the monostatic RCS. The RCS measured by the radar at angles $\theta_i \neq \theta_s$ and $\varphi_i \neq \varphi_s$ is called the bi-static RCS.

We can express the scattered electric field in the far zone as

$$E_s = \frac{e^{-ikr}}{kr}\{F_\theta(\theta,\varphi)\hat{\theta}+F_\varphi(\theta,\varphi)\hat{\varphi}\} \tag{3.16}$$

Where

$$F_\theta(\theta,\varphi) = -\sum_{m=1}^{\infty}\sum_{n=m}^{\infty}\{\iota^{n+1} * \frac{mS_{mn}(\gamma,\cos(\theta))}{\sin(\theta)} * [a_n^s\sin(m\varphi) - c_n^s\cos(m\varphi)] - \iota^n\frac{d}{d\theta}(S_{mn}(\gamma,\cos(\theta))) * [d_n^s\sin(m\varphi) + b_n^s\cos(m\varphi)]\} + \sum_{n=0}^{\infty}\iota^n\frac{d}{d\theta}\left(S_{0n}(\gamma,\cos(\theta))\right) * b_n^s(m=0) \tag{3.17}$$

$$F_\varphi(\theta,\varphi) = \sum_{m=1}^{\infty}\sum_{n=m}^{\infty}\{-\iota^n * \frac{mS_{mn}(\gamma,\cos(\theta))}{\sin(\theta)} * [a_n^s\sin(m\varphi) - c_n^s\cos(m\varphi)] - \iota^{n+1}\frac{d}{d\theta}(S_{mn}(\gamma,\cos(\theta))) * [d_n^s\sin(m\varphi) + b_n^s\cos(m\varphi)]\} - \sum_{n=0}^{\infty}\iota^n\frac{d}{d\theta}\left(S_{0n}(\gamma,\cos(\theta))\right) * a_n^s(m=0) \tag{3.18}$$

$(\rho, \theta, \varphi)$ are the spherical coordinates at the point of observation with respect to the center of the spheroid.

The normalized bi-static cross-section is given by

$$\frac{\pi * \sigma(\theta,\varphi)}{\lambda^2} = |F_\theta(\theta,\varphi)|^2 + |F_\varphi(\theta,\varphi)|^2 \quad (3.19)$$

The normalized backscattering cross-section is obtained from above equation by substituting $\theta = \theta_i$ and $\varphi = 0$.

$$\frac{\pi * \sigma(\theta)}{\lambda^2} = |F_\theta(\theta_i, 0)|^2 + |F_\varphi(\theta_i, 0)|^2 \quad (3.20)$$

## 4. Numerical Results and Discussion

After a large number of numerical calculations, the results are presented in the form of normalized bi-static and backscattering cross-sections for various spheroid sizes, M values, coating thicknesses, and coating permittivity and permeability. From the results of these calculations some interesting conclusions concerning the polarization and symmetry properties of the solutions can be drawn.
Instead of the parameter M, which extends over an infinite range, we use the dimensionless variable $\alpha$, defined by $\tan\alpha = M\eta_o$

So that $\alpha = 0$ corresponds to the PMC case ($M = \infty$) and $\alpha = 90^\circ$ corresponds to the PEC case ($M = \infty$).

Results are presented in what follows for spheroids of size parameter $\xi_o = 3$ and the coating parameters $\xi_1/\xi_o = 1.1$ Since all the fields have been expanded using infinite series, in order to obtain numerical results, these series have to be truncated appropriately. The series is taken from 0 to 5, i.e., n is taken from 0 to 5.
In order to verify that the analysis and the software used for performing the calculations are correct, we have calculated the normalized backscattering cross-section for a PEMC spheroid of size parameter $\xi_o = 3$ and the coating parameters $\xi_1/\xi_o = 1.1$ and compared these results with the corresponding results obtained for a perfectly conducting sphere of an identical geometry.

1. The variation of normalized backscattering cross-section of co-polarized as well as cross-polarized component of the field scattered from the PEMC spheroid coated by dielectric medium is studied against the admittance parameter M in scattering plane $\phi = 0^\circ$ and scattering angle $\theta = 15^\circ$.

In the figure (2) the core size parameter is $\xi_o = 3$ and the coating parameters $\xi_1/\xi_o = 1.1,\ \varepsilon_r = \mu_r = 0.01$. (a) Total Backscattering cross section (b) Co-Polarized contribution to Backscattering cross section (c) Cross-Polarized contribution to Backscattering cross section. Both the co and cross-polarized contribution is shown along with the total backscattering cross section.

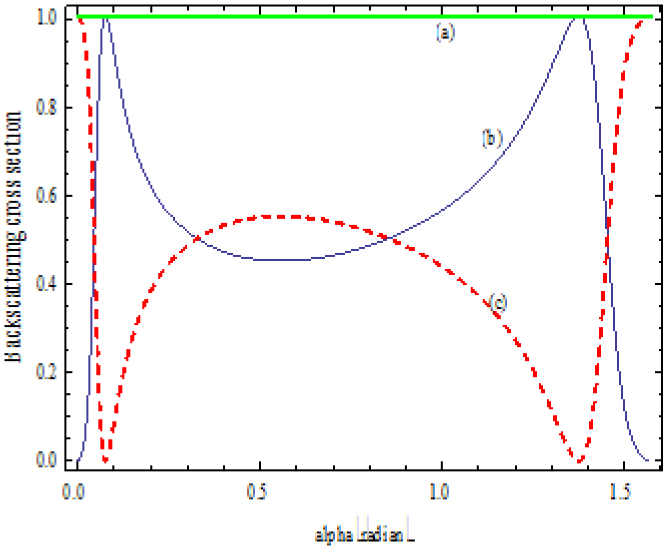


**Figure 2:** Backscattering cross section of a coated PEMC spheroid.

The total Backscattering cross section does not depend on M, but the relative contributions of the co-polarized and cross-polarized contributions depend on M. Both the co-polarized and cross-polarized component of scattered field varies approximately inversely to each other. It means that if one component has increasing values, at the same time the other has decreasing one. Comparing these results in with the corresponding results calculated in (Ruppin 2009) using spherical vector wave functions the two sets of results are in agreement.

2. Variation of normalized bi-static cross-section of the PEMC spheroid with the scattering angle is considered for various PEMC admittances and for TE polarizations of the incident Gaussian Beam. Variation is studied at different admittance angles whereas the scattering phase is kept constant at $\phi = 90^\circ$.

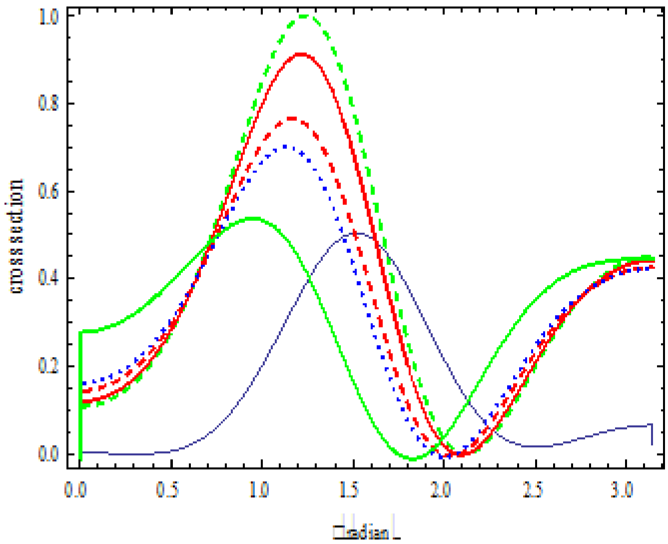


**Figure 3:** Normalized bi-static cross section variation with scattering angle $\theta$.

Above figure (3) shows the variation of normalized bi-static cross section with scattering angle $\theta$ having scattering plane at $\phi = 90^\circ$. This variation is studied at admittance angles

**International Journal of Science and Research (IJSR)**
**ISSN (Online): 2319-7064**
**Index Copernicus Value (2013): 6.14 | Impact Factor (2013): 4.438**

as $\alpha = 0^\circ, 15^\circ, 30^\circ, 45^\circ, 60^\circ, 75^\circ$. The core size parameter is $\xi_o = 3$ and the coating parameters ${}^{\xi_1}/_{\xi_o} = 1.1,\ \varepsilon_r = \mu_r = 0.01$.

As shown in figure (3) the variation of normalized bi-static cross section of PEMC spheroid is shown with scattering angle from $0^\circ$ to $180^\circ$ at different values of admittance parameter M. However the scattering plane is taken $\phi = 90^\circ$ for all the above cases. For α=0 (PMC spheroid) and α=90(PEC spheroid) bi-static cross section is minimum. While increasing α from 0 to 45 bi-static cross section increases at α=45 it is maximum further increasing value of α decreases the bi-static cross section.

3. The variation of normalized backscattering cross section has been studied with the permittivity of dielectric medium for different values of admittance parameter M while keeping scattering angle and permeability of dielectric material constant.

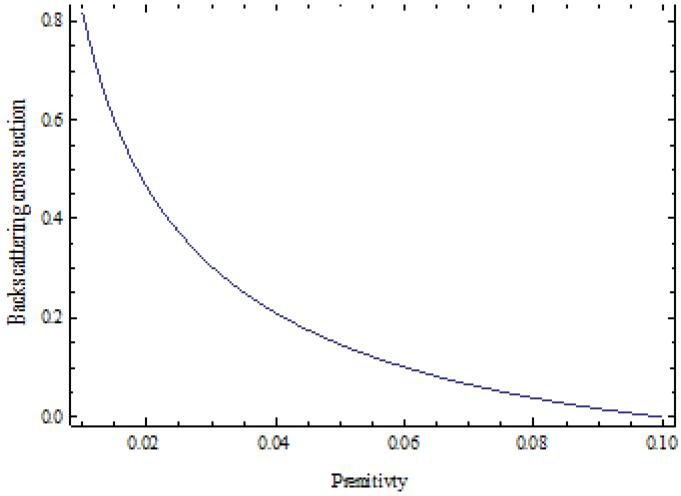


**Figure 4:** Variation of Bistatic cross section with permittivity of dielectric material having admittance angle $alpha = 15^\circ$

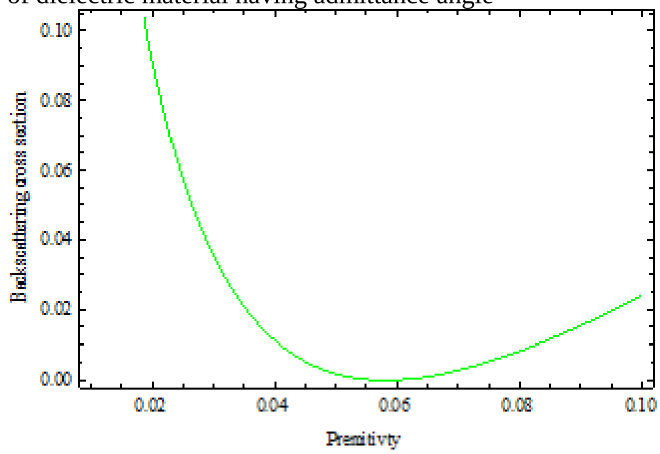


**Figure 5:** Variation of Bistatic cross section with permittivity of dielectric material having admittance angle $alpha = 30^\circ$

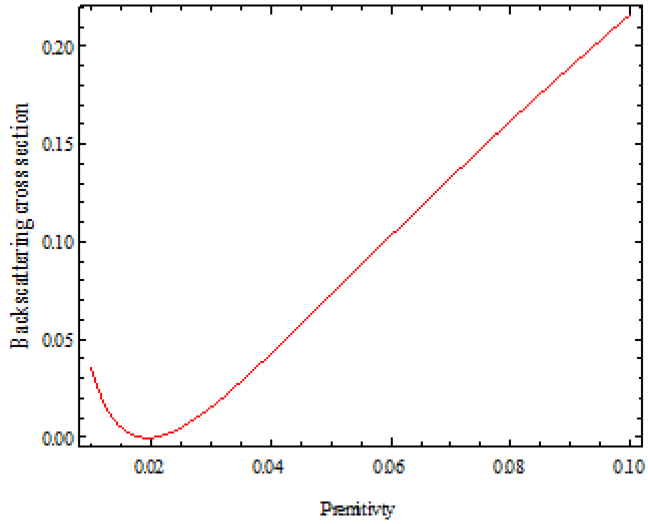


**Figure 6:** Variation of Bistatic cross section with permittivity of dielectric material having admittance angle $alpha = 45^\circ$

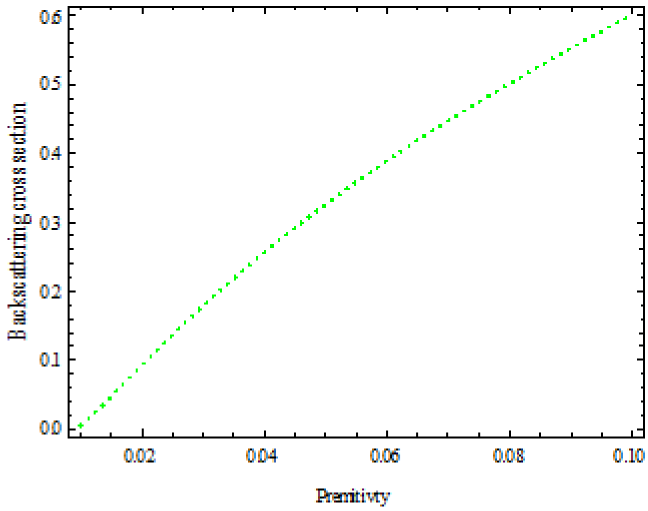


**Figure 7:** Variation of Bistatic cross section with permittivity of dielectric material having admittance angle $alpha = 60^\circ$

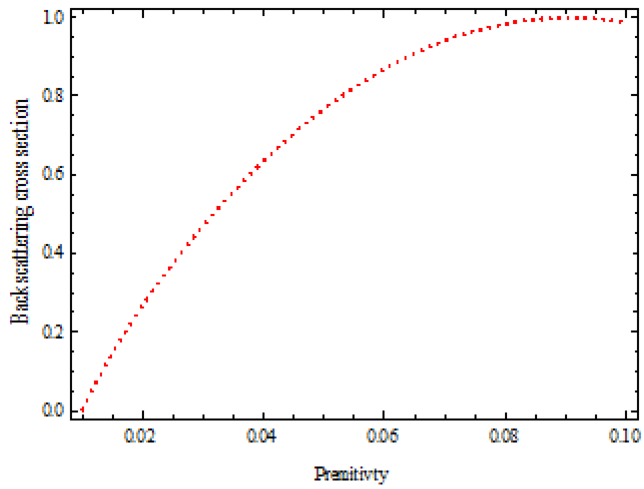


**Figure 8:** Variation of Bistatic cross section with permittivity of dielectric material having admittance angle $alpha = 75^\circ$

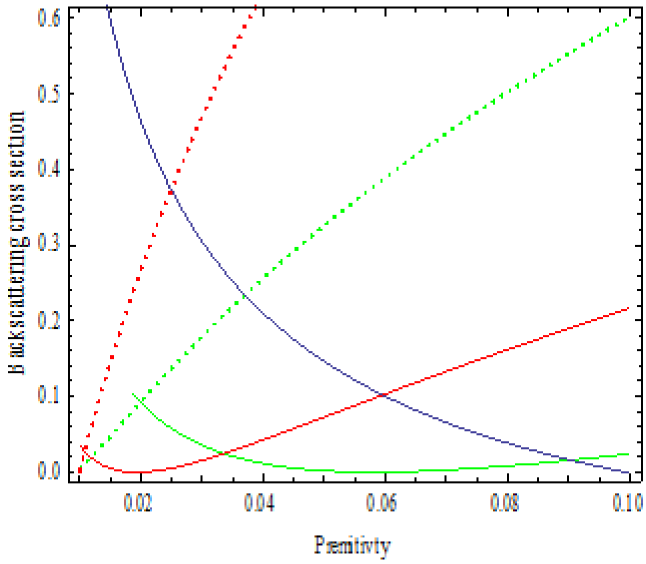


**Figure 9:** Variation of back scattering cross section with permittivity of dielectric material

In figure (9) variation of back scattering cross section with permittivity of dielectric material is shown while having scattering plane $\phi = 90^{\circ}$, scattering angle $\theta = 15^{\circ}$ and permeability $\mu_r = 0.05$.at α=15 back scattering cross section decreases sharply with the increase in permittivity of dielectric material. As admittance angle increases from 15 to 45there is very slight change in back scattering cross section. When admittance angle increases from 45 to 180 back scattering cross section increases sharply with increasing permittivity.

## 5. Conclusion

Analytical expressions have derived to find out the scattering of Gaussian beam by PEMC spheroid coated by a dielectric material. An extended version of classical Mie theory is used which provides us two sets of six equations. By solving these equations we got the values of the scattering and transmitted co-efficient. We have observed that by introducing the dielectric coating around the PEMC spheroid the magnitude of Co and Cross components increases. If we increase the value of M the magnitude of co component decreases, at M=1 (α=45) it is half co polarized and half cross polarized further increase in M decreases the co component. In the cases of changing permittivity of coated dielectric material the resonance of the back scattering cross section of Co and Cross components varies as it is expected from physical consideration.

## References

[1] Ghaffar, N. Mahmood, M. Shoaib, M.Y. Naz, A. Illahi, Q.A. Naqvi, Scattering of a radially oriented hertz dipole field by a perfect electromagnetic conductor (PEMC) sphere, Prog. Electromagnet. Res. B 42 (2012) 163–180.

[2] Lindell, I. V. and A. H. Shilvola. 2005. Perfect electromagnetic conductor. *Journal of Electromagnitic Wave Application*, 19(7): 861-869.

[3] Lindell, I.V. and A. H. Sihvola. 2005. Realization of the PEMC Boundary. *IEEE Transactions on Antennas and Propagation*, 53(9): 3012-3018.

[4] Lindell, I. V. and A. H. Shilvola. 2008.Reflection and Transmission of wave at the interface of Perfect Electromagnetic Conductor.Journal of Electromagnetic Wave Application, 5:169-183

[5] Pendry, J. B., D. Schurig, and D. R. Smith. 2006. Controlling electromagnetic fields. Science, 312: 1780–1782.

[6] Ruppin, R. 2009. Scattering of electromagnetic radiation by a coated perfect electromagnetic conductor sphere. Progress in Electromagnetic Research Letter, 8:53-62.

[7] Ruppin, R. 2006. Scattering of electromagnetic radiation by perfect electromagnetic conductor sphere. Journal of Electromagnetic Waves and Applications, 20: 1569-1576.

## Author Profile

**Bushra Anam Khalil** was born in Faisalabad, Pakistan. She received M.S Degree in Physics from The University of Agriculture Faisalabad, Pakistan and B.Sc Physics from Punjab University Lahore, Pakistan. She is Gold medalist in M.Sc and B.Sc and acquires several scholarships & awards in her academic career. Her major research interest includes: Electrodynamics, Mechanics, Instrumentation and Control.

**M. Waqas Munir** was born in Faisalabad, Pakistan. He received M.S Degree in Control System and Electronics from The University of Teesside, United Kingdom. Also, B.Eng [Honor] in Electrical & Electronics Engineering from The University of Faisalabad, Faisalabad, Pakistan. He is a member of IEEE, PEC, PECongress & IAENG. He is a research scholar and lecturer, work with Engineering Institute. His major research interest includes: Control System, Power Electronics & Signal Processing.

**Syed Ali Shahid** is a master degree holder in computer science. He has the experience of around five years in teaching in both public sector and private sector institution. The basic interest of the writer is computational physics and quantum computing.